THE JOURNAL OF BIOLOGICAL CHEMISTRY
Vol. 273, No. A5, Issue of August 14, pp. 21298–21308, 1998

Printed in U.S.A.

Activation of Gene Expression by a Novel DNA Structural Transmission Mechanism That Requires Supercoiling-induced DNA Duplex Destabilization in an Upstream Activating Sequence*

(Received for publication, January 28, 1998, and in revised form, May 7, 1998)

Steven D. Sheridan‡§, Craig J. Benham¶, and G. Wesley Hatfield‡‖

From the ‡Department of Microbiology and Molecular Genetics, College of Medicine, University of California, Irvine, California 92697 and the ¶Department of Biomathematical Sciences, Mount Sinai School of Medicine, 1 Gustave Levy Place, New York, New York 10029

We have previously demonstrated that integration host factor (IHF)-mediated activation of transcription from the *ilv*P_G promoter of *Escherichia coli* requires a supercoiled DNA template and occurs in the absence of specific interactions between IHF and RNA polymerase. In this report, we describe a novel, supercoiling-dependent, DNA structural transmission mechanism for this activation. We provide theoretical evidence for a supercoiling-induced DNA duplex destabilized (SIDD) structure in the A + T-rich, *ilv*P_G regulatory region between base pair positions +1 and −160. We show that the region of this SIDD sequence immediately upstream of an IHF binding site centered at base pair position −92 is, in fact, destabilized by superhelical stress and that this duplex destabilization is inhibited by IHF binding. Thus, in the presence of IHF, the negative superhelical twist normally absorbed by this DNA structure in the promoter distal half of the SIDD sequence is transferred to the downstream portion of the SIDD sequence containing the *ilv*P_G promoter site. This IHF-mediated translocation of superhelical energy facilitates duplex destabilization in the −10 region of the downstream *ilv*P_G promoter and activates transcription by increasing the rate of open complex formation.

Negative superhelicity imposed on a DNA domain can drive local transitions to several types of alternate DNA conformations. These include cruciform extrusion at inverted repeat sequences, Z-DNA at alternating purine-pyrimidine sequences, and denaturation (also called local melting) that concentrates at A + T-rich sites (1–3). Each of these transitions requires free energy, and each releases free energy because the change of local helicity that occurs upon formation partially relaxes the imposed superhelicity. In a domain containing a single susceptible site, the transition will occur when the energy released exceeds the energy required to perform the transition (4).

In domains that contain multiple sites that are susceptible to transition, a complex competition among them will occur (1, 5). Whether a specific transition occurs depends not just on its local sequence but also on how well that transition competes with all others elsewhere in the domain. For example, David Lilley and colleagues (2) showed that the melting transition of an A + T-rich region contained within a supercoiled DNA plasmid required a significantly higher level of negative supercoiling when a $(TG)_{12}$ region able to form left-handed Z-DNA under superhelical tension was inserted into the plasmid. This shows that the presence of a more susceptible site can inhibit less favorable transitions at other positions. In other words, superhelix-induced structures compete with one another for the negative superhelical energy required for their formation.

The transition behavior of superhelical domains also may be influenced by proteins that bind at or near these transition sites. For example, if a DNA region that is favored to form a superhelix-induced alternate structure is trapped in the B-form by the binding of a protein, the transition may be transferred to another region in the domain. If this second site is the −10 region of a promoter, this translocation of destabilization of the B-form can be used to activate transcription initiation by facilitating open promoter complex formation. In this report, we present evidence for this type of a DNA structural transmission mechanism for the regulation of gene expression in *Escherichia coli*.

Integration host factor (IHF)[1] binds to an upstream activating sequence (UAS1) and activates transcription from the downstream *ilv*P_G promoter of the *ilvGMEDA* operon of *E. coli*. This activation occurs in the absence of specific protein interactions between IHF and RNA polymerase, is not the consequence of a DNA looping mechanism, and requires a superhelical DNA template (6–8). IHF binding in the UAS1 region of a superhelical DNA template results in duplex destabilization in the −10 region of the downstream *ilv*P_G promoter site. This DNA structural change at the downstream promoter site is correlated with an increase in the rate of open complex formation and a concomitant increase in the rate of transcription initiation (7). In this report, (i) we provide theoretical evidence for a supercoiling-induced DNA duplex destabilized (SIDD) structure in the A + T-rich, *ilv*P_G regulatory promoter region between bp positions +1 and −162; (ii) we present experimental evidence to show that the local B-form DNA structure in the UAS1 region immediately upstream of the IHF binding site is destabilized by superhelical stress; (iii) we show that IHF binding prevents this duplex destabilization; (iv) we show that the threshold superhelical densities required for IHF activation and for the destabilization of this upstream portion of the SIDD region in UAS1 are similar; and (v) we demonstrate that the presence of this upstream destabilized structure is required for

* This work was supported in part by National Science Foundation Grants MCB-9723452 (to G. W. H.) and BIR-93–10252 (to C. J. B.) and National Institutes of Health Grants GM55073 (to G. W. H.) and GM47012 (to C. J. B.). The costs of publication of this article were defrayed in part by the payment of page charges. This article must therefore be hereby marked "*advertisement*" in accordance with 18 U.S.C. Section 1734 solely to indicate this fact.

§ Supported by U.S. Public Health Service Training Grant GM07311.

‖ To whom correspondence should be addressed. Tel.: 949-824-5858; Fax: 949-824-8598; E-mail: gwhatfie@uci.edu.

[1] The abbreviations used are: IHF, integration host factor; UAS, upstream activating sequence; SIDD, supercoiling-induced duplex destabilization; bp, base pair(s); ΔLk, linking number difference; σ, superhelical density.

IHF activation and IHF-mediated duplex destabilization in the −10 region of the downstream promoter. These observations suggest a novel, superhelically dependent DNA structural transmission mechanism of the type described above; *i.e.* binding of IHF prevents the superhelical destabilization of the upstream region but promotes duplex destabilization in the −10 region of the *ilv*P_G promoter at the other end of the SIDD structure. This IHF-mediated duplex destabilization in the −10 region of the *ilv*P_G promoter lowers the energy of activation for open complex formation and increases the rate of transcription initiation (7). This mechanism accounts for the facts that IHF activation of transcription from the *ilv*P_G promoter is DNA supercoiling-dependent and occurs in the absence of specific interactions with RNA polymerase.

MATERIALS AND METHODS

Chemicals and Reagents—Restriction endonucleases, T4 DNA ligase and T4 polynucleotide kinase were purchased from New England Biolabs. *E. coli* RNA polymerase, pancreatic RNasin, and DNase I were purchased from Boehringer Mannheim. Radiolabeled nucleotides were obtained from NEN Life Science Products. Osmium tetroxide (OsO_4), potassium permanganate ($KMnO_4$), and 2,2′-bipyridine were purchased from Sigma. DNA probes were radiolabeled using a nick translation kit purchased from Amersham Pharmacia Biotech. DNA sequencing was performed using the Sequenase™ kit of U.S. Biochemical Corp. DNA oligonucleotides were purchased from Operon Inc. Integration host factor was purified in this laboratory by the method of Nash *et al.* (28).

Plasmids and Bacterial Strains—Plasmid DNA isolation and all recombinant DNA manipulations were carried out using standard methods (29, 30). Plasmids used in this study are described in Table I.

Determination of IHF Binding Affinity to the Wild Type and Mutant ilvP_G UAS1 Regions—Gel mobility shift assays with linear DNA fragments containing the IHF target site in the UAS1 region upstream of the *ilv*P_G promoter were employed to determine the binding affinity of IHF. For the wild type UAS1 region, a 471-bp *Eco*RI–*Bam*HI DNA fragment containing the *ilv*P_G promoter region from *ilv* bp position −248 to +6 (9) was isolated from plasmid pDHΔwt (Table I) and radiolabeled at each 5′-end with T4 polynucleotide kinase and 10 μCi of [γ-^{32}P]ATP (6,000 Ci/mmol). The binding affinity of IHF to the UAS1 region with the upstream half of the A + T-rich sequence in the UAS1 region deleted was determined on a 269-bp *Bst*YI–*Bam*HI DNA fragment containing the *ilv*P_G promoter region from −98 to +6 (9) isolated from plasmid pSSΔ98 (Table I). The radiolabeled DNA (1×10^{-11} M final concentration) was preincubated with purified IHF in a 20-μl assay mixture (40 mM Tris-HCl (pH 8.0), 4 mM $MgCl_2$, 70 mM KCl, 0.1 mM EDTA, and 0.1 mM dithiothreitol). The free IHF concentration in each sample was assumed to be the same as the total IHF concentration, since the DNA template concentration was significantly lower than the K_d for IHF binding. DNA fragments and IHF were incubated at 25 °C for 20 min, and the free and IHF-bound DNA fragments were separated by electrophoresis on a 5% polyacrylamide gel (4.83% acrylamide, 0.17% *N,N′*-methylenebisacrylamide) in TAE buffer (40 mM Tris acetate (pH 8.0), 1 mM EDTA) (29). Electrophoresis was performed at 25 °C. Free and IHF-bound DNA fragments were visualized by autoradiography following multiple time exposures of the dried gels to Kodak XAR-5 film at −70 °C in the presence of a Cronex Quanta III intensifying screen (DuPont). Quantitation of band intensity on autoradiographic film was performed utilizing the public domain NIH Image gel quantitation software.[2] Determination of equilibrium binding constants (K_B) was performed by fitting the binding curve to the Langmuir isotherm, $Y = k[P]/1 + k[P]$, where k is the equilibrium binding constant and [P] is the free protein concentration with Sigmaplot version 4.17 software by Jandel Scientific Corp.

DNase I Footprinting of IHF Binding to Wild Type and Mutant UAS1 Regions of ilvP_G—DNase I footprinting assays were performed to determine the location of IHF binding in the *ilv*P_G promoter-regulatory region of various constructs contained on a negatively supercoiled DNA template. Supercoiled plasmid DNA (1×10^{-9} M final concentration; $\sigma = -0.06$) was incubated for 20 min at 25 °C in the absence or presence of purified IHF (30 nM final concentration) in the same assay mixture used for the gel mobility shift assays. The IHF/DNA mixture was treated with 5 ng of DNase I for exactly 2 min to ensure single-hit kinetic conditions (8). DNase I reactions were stopped by placing the samples in boiling water for 5 min. The DNA was collected by precipitation with 2-propanol and resuspended in distilled water. Sites of DNase I-specific cleavage were visualized by the primer extension analysis described below with single-stranded DNA oligonucleotide primers that anneal to *ilv* DNA sequences 5′ (*ilv* bp positions −207 to −187 or −160 to −132) or 3′ (vector-specific bp positions +62 to +32 relative to the *ilv*P_G transcriptional start site) (9) of the UAS1 and *ilv*P_G promoter regions on the nonsense and sense strands, respectively.

Mung Bean Nuclease Assays—1.0 μg of supercoiled plasmid DNA template was digested with mung bean nuclease (0.1 units) in a 50-μl reaction (45 mM Tris borate (pH 7.6), 1 mM $ZnCl_2$, and 1 mM EDTA) for 15 min at 37 °C as described (3). The reaction was quenched by two extractions with phenol/chloroform/isoamyl alcohol followed by a single extraction with chloroform. The DNA was collected by precipitation with 2-propanol and resuspended in distilled water. The sites of mung bean nuclease sensitivity were resolved using primer extension mapping as described below with single-stranded DNA oligonucleotide primers that anneal to *ilv* DNA sequences 5′ (*ilv* bp positions −207 to −187) (9) of the UAS1 and *ilv*P_G promoter regions on the nonsense strand.

Osmium Tetroxide Probing Assays—1.0 μg of supercoiled plasmid DNA template was treated with 2 mM osmium tetroxide (OsO_4) in the presence of 2 mM 2,2′-bipyridine in a 50-μl reaction (45 mM Tris borate (pH 7.6) and 1 mM EDTA) at 37 °C. After 5 min, the reaction was stopped by precipitation with isopropyl alcohol, and the DNA pellet was collected by centrifugation. The pellet was dried, resuspended in distilled water, and reprecipitated with isopropyl alcohol. The collected pellet was washed with 70% ethanol, collected, and dried. The final pellet was resuspended in distilled water. The sites of OsO_4 modification were resolved using primer extension mapping as described below with the single-stranded DNA oligonucleotide primers described above.

Potassium Permanganate Probing Assays—1.0 μg of supercoiled plasmid DNA was treated with 3 mM potassium permanganate in a 50-μl reaction (45 mM Tris borate (pH 7.6) and 1 mM EDTA) at 37 °C. After exactly 4 min, the reaction was stopped by the addition of 3 μl of β-mercaptoethanol. The modified DNA was precipitated with isopropyl alcohol, collected by centrifugation, washed twice with 70% ethanol, and dried. The final pellet was resuspended in distilled water. The sites of $KMnO_4$ modification were resolved using primer extension mapping as described below with the single-stranded DNA oligonucleotide primers described above.

Base Pair Resolution Mapping of Chemical Modification and Nuclease-specific Cleavages—The sites of chemical modification and nuclease cleavage described above were mapped by primer extension using T7 DNA polymerase and *ilv*-specific oligonucleotides. After nuclease or chemical treatment, the DNA plasmid template was denatured in the presence of 200 mM NaOH for 10 min at 37 °C. 100 ng of an oligonucleotide primer was added, and the DNA was renatured with 300 mM NaOAc (pH 5.2). The reannealed DNA was precipitated with isopropyl alcohol, washed once with 70% EtOH, collected, and dried. The DNA pellet was resuspended in reaction buffer (40 mM Tris-HCl (pH 7.5); 20 mM $MgCl_2$; 50 mM NaCl; 300 nM each dGTP, dCTP, and dTTP; 1 mM dithiothreitol; and 10 μCi of [α-^{32}P]dATP (3,000 Ci/mmol)). 1 unit of T7 DNA polymerase was preincubated in this reaction mixture for 5 min. The polymerization reaction was initiated with the addition 2.5 μl of buffer containing a 100 μM concentration of each dNTP in distilled water. The reaction was allowed to continue for 5 min at 25 °C until it was stopped by the addition of an equal volume of stop buffer (95% formamide, 5 mM EDTA, 0.025% each bromphenol blue and xylene cyanol).

In order to determine the base pair location of modified and cleaved sites, primer extension for dideoxy sequencing was performed as described above with 1.0 μg of untreated plasmid DNA and the same *ilv*-specific oligonucleotide primers except for the addition of the appropriate ddNTP (10 μM) to the initiation buffer. The primer extension products were separated by electrophoresis on an 8% denaturing polyacrylamide gel (7.6% acrylamide, 0.4% *N,N′*-methylenebisacrylamide) containing 8 M urea in TBE buffer (90 mM Tris borate (pH 8.0), 1 mM EDTA) and visualized by autoradiography following exposure of the gels to Kodak XAR-5 film at −70 °C in the presence of a Cronex Quanta III intensifying screen (DuPont).

In Vitro Transcriptions—The closed circular supercoiled plasmids pDHΔwt and pSSΔ98 (Table I) were used as DNA templates for *in vitro* transcription assays performed in the absence and presence of purified IHF protein. RNA polymerase-plasmid DNA complexes were formed by preincubating 0.5 units (1.2 pmol) of RNA polymerase and 250 ng of plasmid DNA (0.1 pmol) in a 45-μl reaction mixture (0.04 M Tris-HCl (pH 8.0), 0.1 M KCl, 0.01 M $MgCl_2$, 1.0 mM dithiothreitol, 0.1 mM EDTA,

[2] Available on the Internet at ftp://zippy.nimh.nih.gov.

200 μM CTP, 20 μM UTP, 10 μCi of [α-^{32}P]UTP (3,000 Ci/mmol), 100 μg/ml bovine serum albumin, and 40 units of RNasin) for 10 min at 25 °C. Transcription reactions were initiated by the addition of 5 μl of a 2 mM ATP, 2 mM GTP solution. Reactions were terminated after 2, 4, 6, 8, and 10 min by removing a 10-μl sample into 10 μl of stop solution (95% formamide, 0.025% bromphenol blue, 0.025% xylene cyanol). The reaction products were separated by electrophoresis on an 8% denaturing polyacrylamide gel (7.6% acrylamide, 0.4% *N,N′*-methylenebisacrylamide) containing 8 M urea in TBE buffer and visualized by autoradiography following exposure of the gels to Kodak XAR-5 film at −70 °C in the presence of a Cronex Quanta III intensifying screen (DuPont).

Generation of Plasmid DNA Topoisomers—10 μg of each plasmid was treated with 20 units of *Drosophila melanogaster* topoisomerase II in a 40-μl reaction mixture (10 mM Tris-HCl (pH 7.9), 50 mM NaCl, 50 mM KCl, 5 mM $MgCl_2$, 0.1 mM EDTA, 15 μg/ml bovine serum albumin, 1 mM ATP, and ethidium bromide (0–20 μM)) for 5 h. Each plasmid DNA sample was extracted three times with phenol to remove the ethidium bromide, precipitated with 2 volumes of isopropyl alcohol, and resuspended in 100 μl of TE (10 mM Tris (pH 8.0) and 1 mM EDTA). The plasmid DNA topoisomers were resolved by electrophoresis on four 1.4% agarose gels in TAE buffer containing 0.006, 0.02, 0.04, or 0.08 μg/ml ethidium bromide. The average linking number difference of the DNA plasmid in each sample (Δ*Lk*) was determined by the band counting methods of Keller (31) and Singleton and Wells (32). The average superhelical density ($-\sigma$) was calculated using the equation $\sigma = -10.5(\Delta Lk/N)$, where N is the number of base pairs in the plasmid (pDHΔwt and pSSΔ98 contain 4203 and 3860 bp, respectively).

Two-dimensional Gel Electrophoresis of Plasmid DNA Topoisomers—A 20-μl sample containing a mixture of 0.2 μg of each topoisomer set created above was mixed with 2 μl of a stock loading buffer containing 50% glycerol and 10 mg/ml xylene cyanol. This topoisomer mixture typically contained plasmid DNAs with superhelical densities ranging from $\sigma = 0.00$ to approximately $\sigma = -0.10$. The sample was loaded into a single circular well (radius = 2 mm) of 24 × 24-cm 1.4% agarose gels prepared with 0.5× TBE (45 mM Tris borate, pH 8.0, 0.5 mM EDTA). Electrophoresis of each gel in the first dimension was performed in 0.5× TBE buffer at 2.5 V/cm at 37 °C for 28 h with constant buffer recirculation at a rate of at least 1 liter/h. Each gel was removed and soaked in 1× TAE buffer (40 mM Tris acetate, pH 8.0, 1.0 mM EDTA) containing different amounts of interchelating dye (0.02–0.08 μg/ml ethidium bromide) for 6–8 h. Each gel was electrophoresed in a direction 90° to the first dimension in the running buffer used to soak the gel. DNA supercoil-dependent structures were evaluated as described by Bowater *et al.* (12).

Generation of Predicted Stress-induced Duplex Destabilization Profiles—The transition properties of superhelical DNA molecules were calculated using a statistical mechanical analysis that evaluates the equilibrium properties of a population of identical, superhelically stressed DNA molecules in which every base pair is regarded as being susceptible to denaturation (1, 5, 10, 33). All states are examined individually, and the cumulative influence of the high energy states is estimated by a density of states calculation. In each state, the superhelical constraint is divided among three deformations, the change of helicity consequent to denaturing the collection of base pairs that are open in that state, helical interwinding of the two strands comprising the resulting denatured region(s), and the residual superhelicity that remains to stress the molecule. The free energies associated with these deformations have been determined by experimental observation. Copolymeric denaturation energetics are assumed, in which the free energy of opening a base pair depends only on whether it is AT or GC. The other energy parameters are given the values that have been found to pertain under experimental conditions in which T = 37 °C, pH = 7.0, and the DNA is placed in a low ionic strength buffer containing 10 mM Tris-HCl and 1 mM Na_2EDTA. Under these experimental conditions, comparison with experimental observations has shown the results of these calculations to be quantitatively accurate. We note that the pH and ionic conditions of the OsO_4 and nuclease digestion experiments reported here are somewhat different that those assumed in the calculations.

Here the results of calculations are depicted as destabilization profiles. The free energy $G(x)$ that is required to assure opening of the base pair at position x is calculated for each position in the DNA sequence. Low values of $G(x)$ occur at positions where the base pair is substantially destabilized, whereas high values are found when the base pair is not destabilized by the imposed superhelical stresses. Destabilization profiles provide more information than plots of opening probability *versus* position, because they also show sites where the duplex is substantially destabilized but not sufficiently to cause denaturation with high probability. Such sites can be biologically important if another process or molecule can provide only an incremental amount of free energy to the opening reaction.

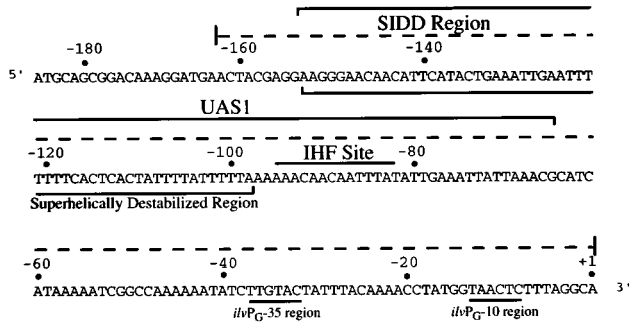

FIG. 1. **Nucleotide sequence of the *ilv*P_G promoter-regulatory region of the *ilvGMEDA* operon of *E. coli*.** The nucleotide sequence of the *ilv*P_G promoter region from bp −185 to +1 is shown. The nucleotides are numbered corresponding to the transcriptional start site from the *ilv*P_G promoter. The IHF core binding site, 5′-AAACAACAATTTA-3′, in the upstream activating sequence UAS1 is located between bp −82 and −96 as indicated. The −10 and −35 hexamer nucleotide regions of the *ilv*P_G promoter are *underlined*. The SIDD region (+1 to −162) is identified by the *dashed bracket*, and the superhelically destabilized region in the UAS1 (−98 to −153) as determined by OsO_4 probing is identified by a *bracket*.

RESULTS

SIDD Is Predicted to Occur in the UAS1 Region at a Physiological Superhelical Density—The base pair composition of the *ilv*P_G promoter-regulatory region is exceptionally A + T-rich (Fig. 1). The 80-bp segment from bp positions −67 to −153 is approximately 88% A + T (9). In order to predict the stability of this region under superhelical stress, DNA SIDD profiles (1, 10) were calculated for plasmid pDHΔwt. This plasmid contains the *ilv*P_G promoter region from bp position −248 to +6 (9) in a pBR322-based vector containing transcriptional terminators located downstream of the *ilv*P_G start site (Table I). Calculations were performed using the energy parameters appropriate for the nuclease digestion procedure of Kowalski (1, 3). The results of these calculations are presented in Fig. 2, *A* and *B*. These are destabilization profiles, plots of the incremental free energy, $G(x)$, required to guarantee denaturation of the base pair at position x. The smaller the value of $G(x)$, the greater the destabilization experienced by that base pair. Values near 0 occur at sites where the B-form DNA base pair interactions are almost completely destabilized. The calculation profiles show that the DNA duplex in the UAS1 region is predicted to be destabilized in this plasmid at a physiological superhelical density of $\sigma = -0.05$. In fact, the predicted DNA destabilization of the UAS1 region in this plasmid context is even more pronounced than the well characterized melting transition of the A + T-rich sequence around bp position 3100 in the 3′-region of the β-lactamase gene (3). A close up view of the UAS1-*ilv*P_G promoter region of this SIDD profile is shown in Fig. 2*C*. These data show that the DNA duplex in the promoter region is predicted to be more stable than it is in the upstream UAS1 region.

Physical Evidence for Superhelically Induced Duplex Destabilization in the UAS1 Region—The SIDD profile for pDHΔwt (Fig. 2), predicts duplex destabilization in the *ilv*P_G promoter-regulatory region at a physiological superhelical density ($\sigma = -0.05$). This prediction was tested by chemically and enzymatically probing the DNA structure of this region in a set of pDHΔwt DNA topoisomers, each prepared at a defined superhelical density. Each plasmid topoisomer was treated in the absence or presence of IHF with osmium tetroxide (OsO_4), which modifies thymine residues in DNA regions where the

TABLE I
Plasmids

Plasmids	Description	Reference
pDD3	Contains a 495-bp *Eco*RI–*Sal*I restriction endonuclease DNA fragment encoding an unique *Bam*HI site, flanked on either side by *rrnB*T_1T_2 terminator sequences, ligated into the *Eco*RI and *Sal*I sites of pBR322.	8
pDHΔwt	Contains a 272-bp *Eco*RI–*Bst*BI (end-filled) restriction endonuclease DNA fragment (*ilv* bp positions −248 to +6)[a] ligated into the unique *Eco*RI–*Bam*HI (end-filled) site of pDD3.	8
pSSΔ-98	Constructed by the removal of a *Ssp*I–*Dra*I restriction endonuclease fragment from plasmid pDHΔwt, end filling, and religation. Contains *ilv* bp positions −98 to +6.[a]	[b]
pSS19Δwt	Contains a 611-bp *Bst*YI–*Bam*HI restriction endonuclease fragment from plasmid pDHΔwt containing *ilv* bp positions −248 to +6[a] ligated into the unique *Bam*HI site of pUC19.	[b]
pSS19Δ-98	Contains a 269-bp *Bst*YI–*Bam*HI restriction endonuclease fragment from plasmid pSSΔ-98 containing *ilv* bp positions −98 to +6[a] ligated into the unique *Bam*HI site of pUC19.	[b]

[a] All *ilv* bp positions are relative to the site of *in vivo* initiation of transcription (+1) from the *ilv*P_G promoter (9).
[b] This work.

helix is in a form that exposes C-5–C-6 bonds (11) or with mung bean nuclease, which cleaves single-stranded DNA (3). OsO_4 reacts with destabilized sites, including premelted or "breathing" regions of A + T-rich DNA sequences, as well as with melted DNA. Nuclease digestion, in contrast, appears only to detect stably denatured regions. The locations of the chemically modified or enzyme-cleaved sites were determined by primer extension analysis as described under "Materials and Methods."

In the absence of IHF, and at average negative superhelical densities between $\sigma = -0.015$ and -0.028 (Fig. 3*A*, *lanes 2* and *3*), OsO_4 reactivity is observed at thymine residues located between bp positions −98 and −116. At average negative superhelical densities of $\sigma = -0.450$ and higher, OsO_4 reactivity spreads to bp position −153 (Fig. 3*A*, *lanes 4–8*). Although primer extension detection of OsO_4 reactivity at the primer distal thymine residues is diminished at the higher superhelical densities, primer extension analysis from the other direction shows that the reactivity of all the thymines in this region on the other strand increases with increasing supercoiling.[3] Thus, it is clear that the boundaries of the destabilized region in UAS1 are at bp positions −98 and −153.

While the results of the calculations presented in Fig. 2 predict superhelically induced duplex destabilization from bp position −70 to −156, the experimental results show that only the promoter-distal portion of this sequence from bp positions −98 to −153 is, in fact, destabilized (Fig. 3). However, given the constraints of the theoretical calculations and the experimental conditions employed here, there is no reason to suppose that these results should be absolutely correlated. The SIDD analyses are based on experimental results obtained in 10 mM Tris-HCl, 1 mM EDTA, pH 8.0 (3). However, in order to correlate the OsO_4 results with the mung bean nuclease digestion and two-dimensional gel electrophoresis analyses reported below, these experiments were performed in the buffer conditions required for electrophoresis (45 mM Tris borate, 0.5 mM EDTA, pH 7.0). Although such differences in ionic strengths between theory and experiments can affect some of the details of the transition, extensive calculations on many sequences have shown that predictions of the regions experiencing destabilization are quite robust, as are the qualitative differences in destabilization among multiple sites. Thus, the predictions of these attributes can be expected to apply under the experimental conditions reported here; but, predictions of the absolute amount of destabilization or the precise extent of denaturation have been shown to be accurate only under the conditions assumed in the calculations.

In order to determine whether or not the OsO_4 pattern is the result of stable unwinding of the DNA helix into a single-stranded form, we treated the plasmid pDHΔwt with single-stranded DNA-specific mung bean nuclease. Unlike OsO_4,

[3] S. D. Sheridan and G. W. Hatfield, unpublished data.

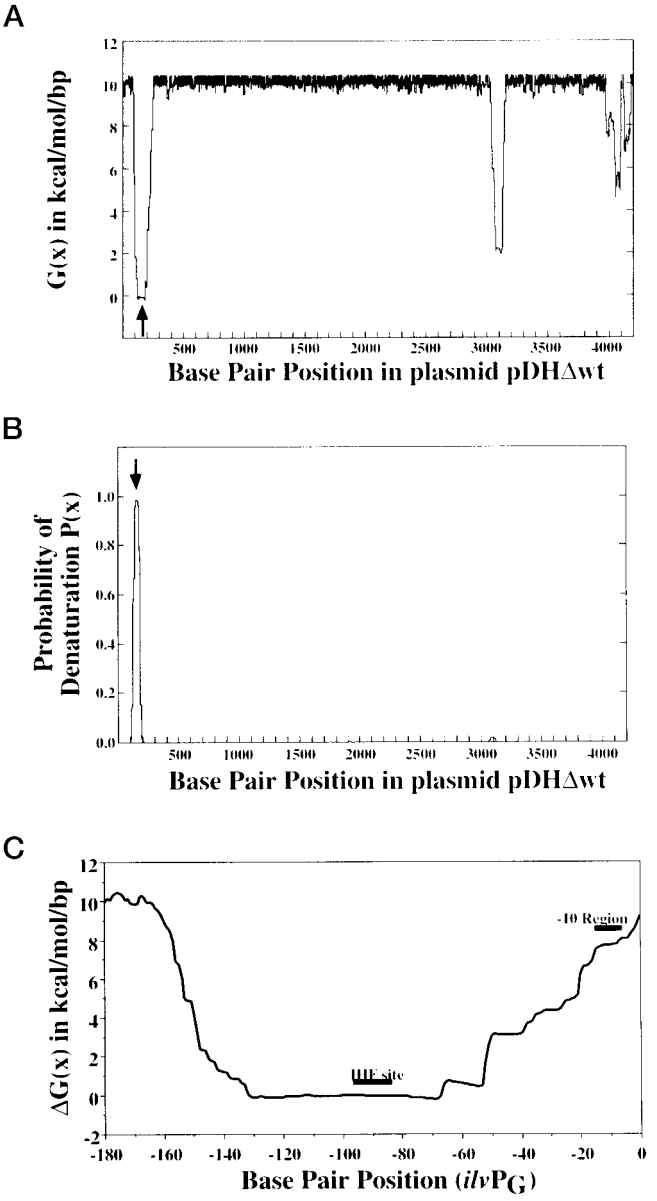

FIG. 2. **SIDD profile of plasmid pDHΔwt at $\Delta Lk = -20$ turns ($\sigma = -0.05$).** *A*, SIDD profile of pDHΔwt indicating the predicted free energy required for DNA duplex destabilization. $G(x)$ is expressed in kcal/mol/bp as a function of base pair location x. The *arrow* indicates the location of the IHF binding site in the UAS1 region of the *ilv*P_G promoter insert (plasmid bp positions 4–256). *B*, probability, $P(x)$, of DNA duplex destabilization as a function of base pair location x. The *arrow* indicates the location of the IHF binding site in the UAS1 region. *C*, close up SIDD profile ($G(x)$) of pDHΔwt from bp position −180 to +1 relative to the *ilv*P_G transcriptional start site (bp positions 76–256 in the plasmid).

mung bean nuclease does not exhibit extensive reactivity in the UAS1 region. Single-stranded nuclease cleavage sites are observed only at base pair positions −112 and −113 (Fig. 3*B*). Thus, complete strand separation only occurs within the central portion of the UAS1 region that has been shown by OsO_4 reactivity to be destabilized by superhelicity. Superhelical densities as high as $\sigma = -0.10$ do not denature the DNA helix throughout this region into a completely single-stranded state. The physical nature of this destabilized structure is currently unknown.

In order to determine the effect of IHF binding on superhelically induced destabilization of the DNA duplex in the UAS1 region, the OsO_4 and mung bean nuclease structural probing experiments were repeated with the same supercoiled plasmid DNA templates in the presence of a saturating concentration (30 nM) of IHF. In the presence of IHF, neither OsO_4 (Fig. 3*C*) nor mung bean nuclease[3] showed any reactivity even at superhelical densities as high as $\sigma = -0.10$. Thus, IHF binding to its target site in the UAS1 region stabilizes the DNA duplex in the upstream UAS1 region, preventing the superhelically induced DNA duplex destabilization that occurs in its absence.

Similar Superhelical Density Thresholds Are Required for IHF-mediated Activation and Superhelically Induced DNA Duplex Destabilization—The superhelical density threshold for IHF-mediated activation of transcription from the *ilv*P_G promoter in pDHΔwt occurs between superhelical densities of $\sigma = -0.03$ and -0.04 (8). If superhelically induced duplex destabilization in the UAS1 region and IHF-mediated activation are functionally correlated, then the threshold superhelical densities required for these two events should be similar. To test this prediction, we employed two-dimensional agarose gel electrophoresis. This method has the ability to accurately determine the threshold superhelical density required to initiate the formation of a superhelically dependent DNA secondary structure to a precision of $\pm\Delta Lk$ of 1 or, in the case of plasmid pDHΔwt, $\pm\sigma = 0.003$ (12). For this measurement, a set of plasmid pDHΔwt topoisomers was created, pooled, and resolved by two-dimensional electrophoresis as described under "Materals and Methods." Fig. 4, *A* and *B*, shows that pDHΔwt exhibits a gradual, DNA superhelically dependent structural transition, beginning at a linking number of $\Delta Lk = -15$. No increase in writhe is observed from a linking number of −16 to the limit of resolution of the gel. This lack of change in writhe over a range of linking numbers is consistent with a gradual untwisting of the DNA helix. However, since the pBR322-based construct, pDHΔwt, contains other superhelically dependent structures (3), we could not be certain that the extension of this transition was due solely to the unwinding of the DNA helix in the UAS1 region. We therefore placed the *ilv*P_G promoter DNA region contained in pDHΔwt (*ilv* bp positions −248 to +6) into the unique *Bam*HI site of pUC19 to create pSS19Δwt (Table I). Since pUC19 does not contain any supercoiling-dependent DNA structures (Fig. 4*C*), only the DNA superhelically destabilized structure in UAS1 is detected in pSS19Δwt (Fig. 4*D*). This UAS1-specific structural transition initiates at a threshold superhelical density of $\sigma = -0.032$. Thus, these experiments demonstrate the initiation of a DNA superhelically induced structural transition in the UAS1 sequence at a threshold superhelical density that correlates well with the superhelical density required for IHF-mediated activation (8).

Deletion of the A + T-rich UAS1 Region Upstream of the IHF Binding Site Eliminates Superhelically Induced Duplex Destabilization in the UAS1 Region—The data presented above demonstrate that the threshold superhelical densities required for IHF-mediated activation of transcription from the *ilv*P_G promoter and the DNA supercoiling-induced duplex destabilization in the UAS1 region are similar. This correlation suggests that destabilization of the DNA duplex in the UAS1 region might be required for IHF-mediated activation. In order to investigate the possibility that these events are functionally related, we created a deletion in which the superhelically destabilized DNA sequence in the UAS1 region was removed without altering the downstream IHF binding site. The UAS1 region upstream of the IHF site in this plasmid (pSSΔ-98; Table I) was replaced with vector DNA of an essentially random base composition (Fig. 5).

The results of mung bean nuclease and OsO_4 structural probing experiments showed that the remaining, promoter-proximal half of the UAS1 region containing the IHF site is insensitive to modification in plasmid pSSΔ-98 at superhelical densities throughout the range of $\sigma = 0.00$ to -0.07.[3] This suggested that the region containing the IHF binding site upstream of the *ilv*P_G promoter in plasmid pSSΔ-98 retains a double-stranded, B-form, DNA structure at superhelical densities that destabilize the full-length UAS1 region in plasmid pDHΔwt. This conclusion is consistent with the results of the two-dimensional gel electrophoresis experiment shown in Fig. 6.

Qualitatively, plasmid pSSΔ-98 does not show the same DNA supercoiling-induced transition as plasmid pDHΔwt (compare Figs. 4*B* and 6*B*). pSSΔ-98 exhibits a transition that initiates at a linking number deficiency of −14 ($\sigma = -0.038$), which we assumed to be the well characterized, unstable region common to pDHΔwt and pSSΔ-98 located around bp position 3100 in the SIDD plot shown in Fig. 2*A* (3). Alternatively, it was possible that the residual transition observed with pSSΔ-98 occurred in the remaining portion of the UAS1 region. To confirm that this was not the case, we transferred the *ilv*-specific sequences in pSSΔ-98 (*ilv* bp positions −98 to +6) into the unique *Bam*HI site of pUC19 to create pSS19Δ-98 (Table I). The results of two-dimensional gel electrophoresis experiments show that plasmids pUC19 (Fig. 4*C*) and pSS19Δ-98 (Fig. 6*A*) do not exhibit any DNA supercoiling-induced structural transitions throughout the superhelical density range assayed ($\sigma = 0.01$ to -0.06). We conclude, therefore, that the gradual DNA superhelically induced DNA duplex destabilization observed in pSS19Δwt is *ilv* UAS1-specific and that this DNA structural transition requires the promoter-distal half of the UAS1 region.

IHF Binds to Its Target Site in the UAS1 Region of pSSΔ-98—Binding sites for IHF consist of a core consensus sequence, WATCAANNNNTTR (where W represents A or T, N represents any base, and R represents pyrimidine), and frequently contain a flanking dA-dT element located immediately upstream of this core sequence (13, 14). Although the functional role of this dA-dT element is unclear, it has been suggested to influence the binding of IHF through indirect contacts with the minor groove of the DNA helix (13, 15). Rice *et al.* (15) have recently analyzed the structure of a co-crystal with the H′ site of phage λ DNA and IHF. They showed that the interaction of IHF with an A tract on the 5′-side of the core sequence is stabilized by the presence of a narrow minor groove created by the poly(dA-dT) sequence and suggested that this interaction is facilitated by structural rather than by sequence specificity. The IHF binding site in the UAS1 region also contains a dA-dT sequence (5′-TATTTATTTTTAAA-3′) on the 5′-side of its core binding sequence. While this sequence is disrupted in pSSΔ-98, an upstream 5′-AATAAA-3′ sequence is retained (Fig. 5*B*). In order to ensure that we had not disrupted the ability for IHF to bind to its core binding site in the UAS1 region, gel mobility shift assays were performed, and the affinities of IHF binding to its target site in the UAS1 region of plasmids pDHΔwt and pSSΔ-98 were compared (Fig. 7). The K_d value for IHF binding

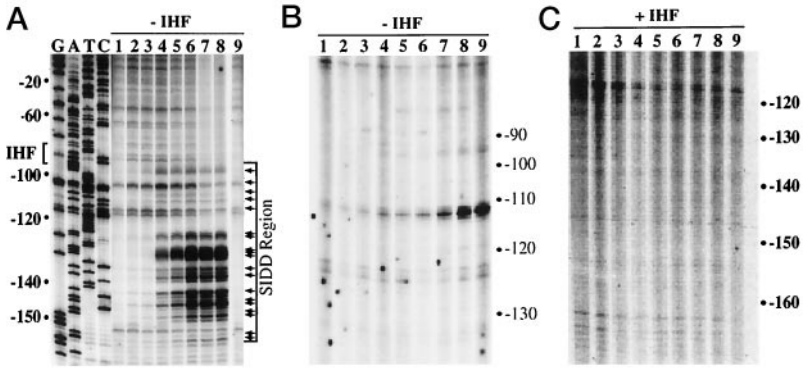

FIG. 3. **Effect of increasing negative superhelical density on chemical and enzymatic reactivity of the *ilv*P_G promoter region on topoisomers of plasmid pDHΔwt in the presence and absence of IHF.** *A* and *C*, topoisomers of plasmid pDHΔwt were treated with 2 mM OsO_4 and 2 mM 2,2-bipyridine, and the sites of modification were mapped to *ilv*P_G-specific bp locations by primer extension as described under "Materials and Methods." Average negative superhelical densities ($-\sigma$) for *A*, *lanes 1–9* (ΔLk = 0 to −40), are σ = 0.00, −0.015, −0.028, −0.045, −0.058, −0.070, −0.085, −0.10, and −0.10. Primer extension analysis in *A*, *lane 9*, was performed on the same topoisomer sample as *lane 8* except that it was not treated with OsO_4. Base pair positions for all primer extension analyses were determined by dideoxy sequencing using the same oligonucleotide primer (*lanes G*, *A*, *T*, and *C*). The *arrows* indicate thymine residues (which correspond to adenines in the other strand in the sequencing ladder) modified by OsO_4. Average negative superhelical densities ($-\sigma$) for *B* and *C*, *lanes 1–9* (ΔLk = 0 to −40), are σ = 0.00, −0.013, −0.025, −0.037, −0.050, −0.063, −0.075, −0.087, and −0.10, respectively. As indicated *above* each *panel*, topoisomers of plasmid pDHΔwt were treated with osmium tetroxide in the absence of IHF except for those presented in *C*, which contained a saturating concentration (30 nM) of IHF. *B*, topoisomers of plasmid pDHΔwt were treated with mung bean nuclease in the absence of IHF, and the sites of nuclease-specific cleavage were mapped to *ilv*P_G-specific bp locations by primer extension. Additional experiments showing OsO_4 modification elsewhere in the plasmid have been performed using a different primer to ensure that the presence of IHF did not squelch the OsO_4 reaction.

was found to be 2.2×10^{-9} M for pDHΔwt and 4.0×10^{-9} M for pSSΔ-98, respectively. In addition, the results of DNase I footprinting experiments on supercoiled plasmids confirmed that IHF binds to the same site on both plasmids.[3] Thus, the deletion of the sequences upstream of the IHF binding site does not eliminate the binding of IHF to its target binding site. We have previously shown that IHF also binds with nearly identical affinities to relaxed and supercoiled DNA templates (8).

Deletion of the A + T-rich UAS1 Region Upstream of the IHF Binding Site Eliminates IHF-mediated Superhelically Induced Duplex Destabilization in the −10 Region of the ilvP_G Promoter—The results of the experiments described above demonstrate that the superhelically destabilized structure in UAS1 is required for IHF-mediated activation. Our proposed mechanism suggests that the IHF-mediated inhibition of the formation of this structure activates transcription by shifting some of the superhelical stress normally absorbed by this structure in the absence of IHF to the downstream *ilv*P_G promoter portion of the SIDD region described above (Fig. 1). If this is the case, then the binding of IHF to plasmid pSSΔ-98, which does not contain the upstream superhelically destabilized structure, should not destabilize the DNA duplex in the −10 region of the downstream *ilv*P_G promoter. This prediction was tested by chemically probing the DNA structure in the −10 region of the *ilv*P_G promoter with $KMnO_4$ and OsO_4 in the presence and absence of IHF on supercoiled pDHΔwt and pSSΔ-98 DNA templates. The results shown in Fig. 8*A* were obtained by primer extension using an oligonucleotide that anneals to *ilv* bp positions −160 to −132 on the transcribed DNA strand. In the presence of IHF, $KMnO_4$ sensitivity is observed at thymines located on the transcribed strand at bp positions −11 and −12 in the promoter region (Fig. 8*A*, *lane 1*). In the absence of IHF, no $KMnO_4$ sensitivity is observed in this region (Fig. 8*A*, *lane 2*). IHF-induced duplex destabilization at these same nucleotide positions is detected with the more sensitive structural probing reagent OsO_4 (Fig. 8*A*, *lane 3*). Again, no destabilization is observed in the absence of IHF (Fig. 8*A*, *lane 4*). Since the upstream primer binding site is not present in pSSΔ-98, a DNA oligonucleotide that binds to a downstream sequence at bp positions 32–62 relative to the *ilv*P_G transcriptional start site on the nontranscribed strand was used for

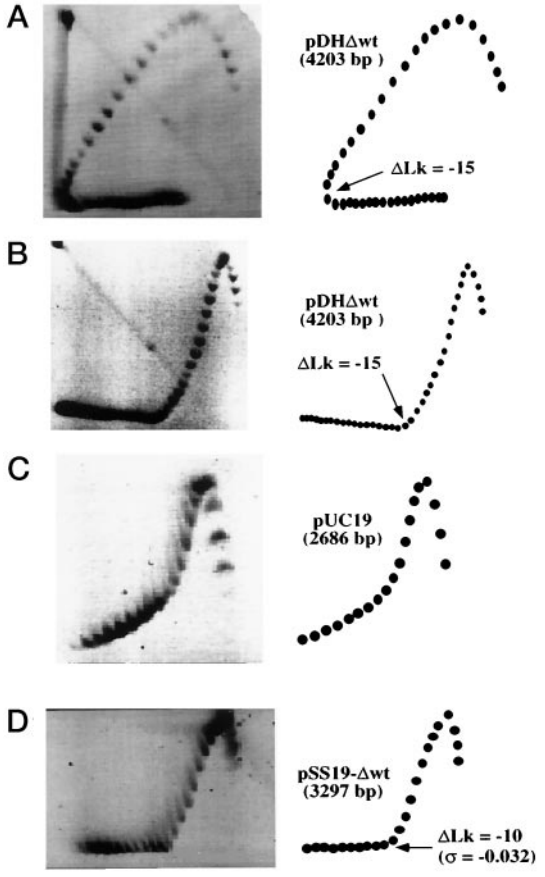

FIG. 4. **Two-dimensional agarose gel electrophoresis of topoisomers of plasmids pDHΔwt, pUC19, and pSS19Δwt.** Plasmid topoisomers of plasmids pDHΔwt (*A* and *B*), pUC19 (*B*), and pSS19Δwt (*D*) were analyzed by two-dimensional agarose gel electrophoresis on a 21-cm 1.4% agarose gel. The first dimension (*top* to *bottom*) was run at 37 °C in 0.5× TBE at 70 V for 28 h. The gels were soaked in 1× TAE buffer containing 0.02 μg/ml ethidium bromide (*A*) or 0.1 μg/ml (*B–D*). The second dimension (from *left* to *right*) was performed in this same buffer at 25 °C until fully resolved. *Tracings* in *A–D* are presented for added clarity. The *arrows* indicate threshold linking number deficiency (and superhelical density ($-\sigma$)) for structural transitions.

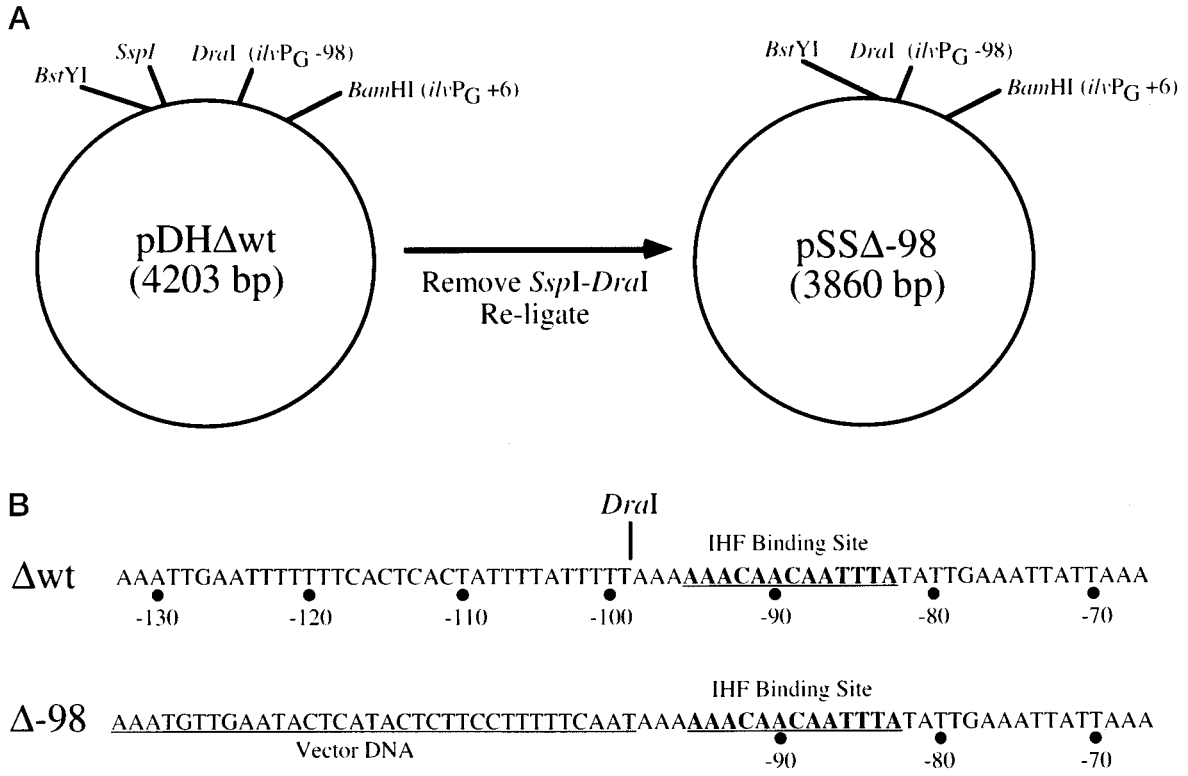

FIG. 5. **Construction of the pSSΔ-98 plasmid and deletion of the UAS1 5′-region.** *A*, diagrams of the plasmids pDHΔwt and pSSΔ-98 used in this study. *B*, nucleotide sequence of the UAS1 region of the *ilv*P_G promoter in these plasmids indicating the location of the IHF core binding site (*underlined* in *boldface type*) and the nucleotide sequence of the vector DNA (*underlined*) that was used to replace the A + T-rich wild type UAS1 5′-region.

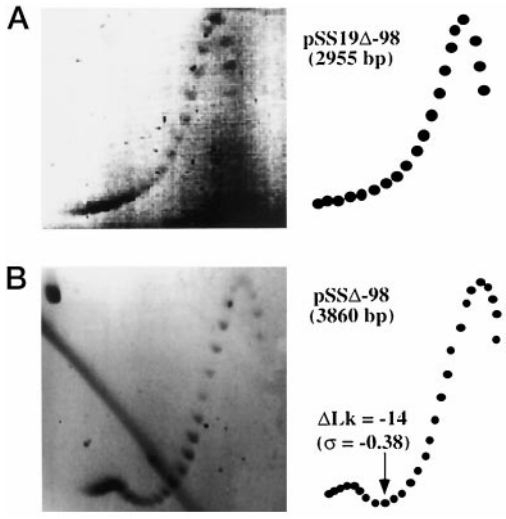

FIG. 6. **Two-dimensional agarose gel electrophoresis of topoisomers of plasmids pSS19Δ-98 and pSSΔ-98.** Topoisomers of plasmids pSS19Δ-98 (*A*) and pSSΔ-98 (*B*) were analyzed by two-dimensional agarose gel electrophoresis on 21-cm 1.4% agarose gels. The first dimension (*top* to *bottom*) was run at 37 °C in 0.5× TBE at 70 V for 28 h. The gels were soaked in 1× TAE buffer containing 0.1 μg/ml ethidium bromide for 6 h. The second dimension (from *left* to *right*) was performed in this same buffer at 25 °C until fully resolved. *Schematic diagrams* for *A* and *B* are presented. The *arrows* indicate threshold linking number deficiency, (Δ*Lk*) (and superhelical density ($-\sigma$)) for structural transitions.

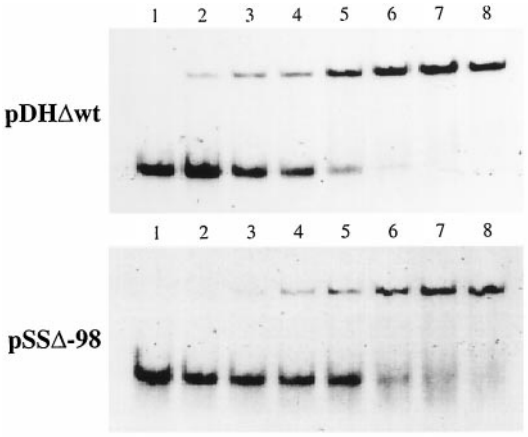

FIG. 7. **Quantitative analysis of IHF binding to its target site in the *ilv*P_G promoter region in pDHΔwt and pSSΔ-98.** Shown are autoradiograms of gel mobility shift assays performed with a γ-^{32}P-end-labeled, 471-bp *Eco*RI–*Bam*HI DNA fragment from plasmid pDHΔwt (containing *ilv* bp from −250 to +6) (*top*) or a 269-bp *Bst*YI–*Bam*HI DNA fragment from plasmid pSSΔ-98 (containing *ilv* bp from −98 to +6) (*bottom*) in the absence (*lane 1*) and increasing concentrations of IHF protein (*lanes 2–8*) as described under "Materials and Methods." IHF concentrations in the binding reactions corresponding to *lanes 2–8* are, respectively, 0.47, 0.94, 1.9, 3.8, 7.5, 15, and 30 nM. DNA concentrations used in these experiments were less than 1×10^{-11} M.

primer extension through the promoter region from the other direction. On this strand, IHF-induced sensitivity on pDHΔwt ($\sigma = -0.06$) is observed at all thymines located between bp positions +7 and −18 (Fig. 8*B*, *lane 1*). However, in the absence of IHF (Fig. 8*B*, *lane 2*) or with pSSΔ-98 in the presence (Fig. 8*B*, *lane 3*) or absence of IHF (Fig. 8*B*, *lane 4*), OsO_4 reactivity at these thymine sites is greatly diminished. These results provide strong evidence that IHF inhibition of duplex destabilization in UAS1 is responsible for IHF activation of duplex destabilization in the *ilv*P_G promoter region.

Superhelically Induced DNA Duplex Destabilization in the UAS1 Region Is Required for IHF-mediated Activation—The results presented above demonstrate that the B-form structure in the upstream half of the UAS1 region is strongly destabilized by negative superhelicity and that this destabilization is inhib-

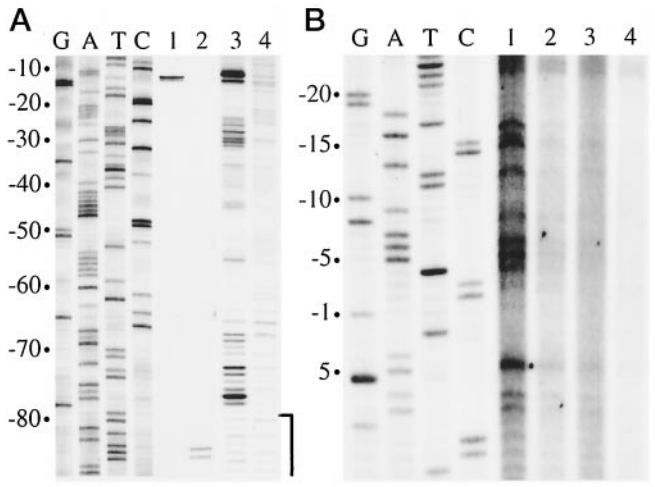

FIG. 8. **Effect of IHF binding in the UAS1 region on the structure of the −10 region of the *ilv*P_G promoter.** *A*, supercoiled plasmid pDHΔwt ($\sigma = -0.06$) was treated with 3 mM KMnO4 (*lanes 1* and *2*) or 2 mM OsO_4 and 2 mM 2,2-bipyridine (*lanes 3* and *4*) in the presence (*lanes 1* and *3*) (30 nM) or absence (*lanes 2* and *4*) of IHF. The *open bracket* indicates the promoter-proximal portion of the IHF binding site. Sites of modification on the transcribed strand of the *ilv*P_G regulatory region were mapped to *ilv*P_G-specific bp locations by primer extension as described under "Materials and Methods." *B*, supercoiled plasmid ($\sigma = -0.06$) pDHΔwt (*lanes 1* and *2*) or plasmid pSSΔ-98 (*lanes 3* and *4*) was treated with 2 mM OsO_4 and 2 mM 2,2-bipyridine in the presence (*lanes 1* and *3*) (30 nM) or absence (*lanes 2* and *4*) of IHF. Sites of modification on the nontranscribed strand of the *ilv*P_G regulatory region were mapped to *ilv*P_G-specific bp locations by primer extension as in *A*.

ited by IHF binding to its target site in the downstream part of this region. A functional correlation between the superhelicity-dependent formation of this structure and the superhelicity dependence of IHF-mediated activation is suggested by the observation that both events occur at similar superhelical densities. This correlation suggests that the formation of this destabilized region might be required for IHF-mediated activation of transcription. The results presented above also demonstrate that a plasmid DNA (pSSΔ-98) with the upstream portion of the UAS1 region deleted in a way that does not eliminate IHF binding cannot form this structure and that IHF binding to this DNA template does not facilitate duplex destabilization in the −10 region of the *ilv*P_G promoter. Therefore, to *finally* determine whether or not this DNA supercoiling-induced structure is required for IHF activation, we performed quantitative *in vitro* transcription experiments in the absence and presence of a saturating concentration of IHF (30 nM) with either pDHΔwt or pSSΔ-98 DNA templates at a superhelical density of $\sigma = -0.07$. The data presented in Fig. 9 show that IHF activates transcription from the downstream *ilv*P_G promoter on pDHΔwt but is unable to activate transcription on plasmid pSSΔ-98, which does not contain a superhelically destabilized site in the upstream UAS1 region and does not exhibit IHF-mediated duplex destabilization in the −10 region of *ilv*P_G, the promoter.

DISCUSSION

In previous reports, we have shown that IHF binding in UAS1 causes the formation of a nucleoprotein structure on a superhelical DNA template that facilitates the destabilization of the DNA duplex in the −10 region of the downstream *ilv*P_G promoter and increases the rate of the isomerization step of the transcription initiation reaction (7). We have also shown that (i) in the absence of IHF, promoter activity increases with increasing DNA supercoiling; (ii) in the presence of IHF, the effect of DNA supercoiling on basal level promoter activity is amplified 5-fold; (iii) IHF binding does not alter the superhelical density of the DNA template; (iv) in the presence or absence of IHF, the relative transcriptional activities of the promoter remain the same at any given superhelical density; (v) IHF activation cannot be replaced by simply increasing the negative superhelical density of the DNA template; and (vi) IHF binds to relaxed and negatively supercoiled DNA templates with nearly identical affinities (8). These results demonstrated that although IHF activation requires a supercoiled DNA template, activation by DNA supercoiling and IHF are effected by separate mechanisms. Therefore, to accommodate these observations and because IHF-mediated activation was shown to occur in the absence of protein interactions between IHF and RNA polymerase, we considered the possibility of activation by a DNA structural transmission mechanism (7, 8).

The experimental results described in this report demonstrate a superhelically induced destabilization of the DNA helix in UAS1. IHF binding is shown to prevent these DNA structural changes. Furthermore, destabilization of this region in the absence of IHF binding is shown to occur at a similar superhelical density threshold required for IHF-mediated activation of transcription from the downstream *ilv*P_G promoter (8). These correlations suggest a DNA structural transmission mechanism for this activation that involves DNA secondary structural transitions (Fig. 10). According to this mechanism, IHF binding in the UAS1 region of a superhelical DNA template inhibits the formation of an untwisted, superhelically induced, alternate DNA structure in which the B-form of the duplex is locally destabilized. In the absence of IHF, this structure is formed under negative superhelicity. In the presence of IHF, the formation of this structure is inhibited. Thus, the superhelicity normally absorbed by this structure in the absence of IHF must be accommodated by transitions at other DNA sites in the presence of IHF. Our experimental results demonstrate that one of these sites is located in the −10 region of the downstream *ilv*P_G promoter where duplex destabilization facilitates open complex formation to activate transcription initiation. This mechanism is consistent with our previous demonstration that IHF binding alters the distribution but not the absolute level of the linking deficiency of a superhelical domain containing the UAS1 region. The experimental evidence reported here in support of this DNA structural transmission mechanism is discussed below.

Theoretical analysis of superhelically induced DNA duplex destabilization (Fig. 2) predicts strong destabilization in the A + T-rich promoter-regulatory region at physiologically relevant superhelical densities. Chemical and enzymatic probing of the structure of the DNA helix demonstrated that duplex destabilization initiates at a low, physiological, superhelical density around bp positions −98 and −116 in the UAS1 portion of this region and spreads about 50 bp to bp position −153 as the negative superhelical density of the DNA template becomes more extreme (Fig. 3*A*). These experiments also showed that although the DNA helix in this region is destabilized, it is not entirely stably unwound (Fig. 3*B*). It is interesting that this superhelically destabilized region is confined to the promoter-distal half of the UAS1 region located immediately upstream of the IHF binding site. It does not extend into the IHF binding site or the farther downstream *ilv*P_G promoter region (Fig. 1). In the presence of IHF, however, no duplex destabilization in the UAS1 region was observed (Fig. 3*C*). In this case, the superhelical deformation absorbed in the absence of IHF by destabilizing this region must be redistributed to other sites. Therefore, since IHF binding has been shown previously to cause DNA superhelicity-dependent duplex destabilization in the −10 region of the downstream promoter (7), it was plausi-

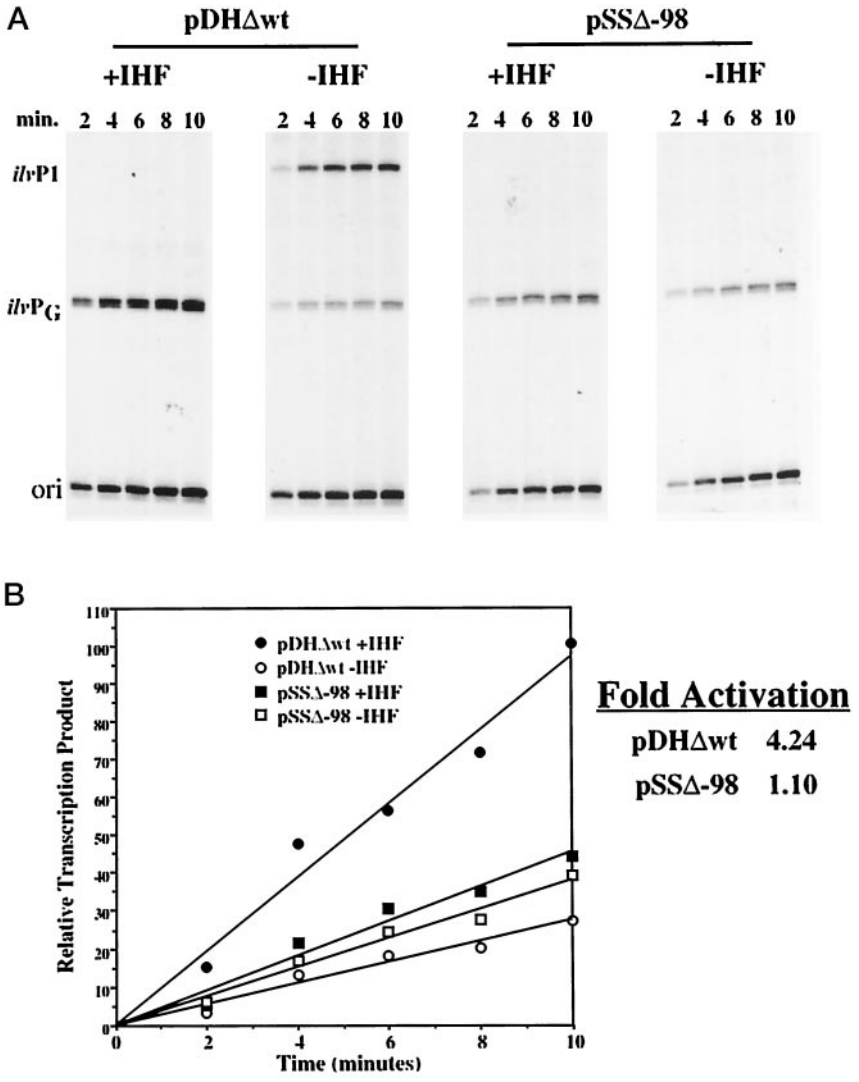

FIG. 9. ***In vitro* transcriptional analysis of *ilv*P_G promoter activity in the absence and presence of IHF on supercoiled plasmids pDHΔwt and pSSΔ-98 ($\sigma = -0.07$).** *A*, *in vitro* transcriptions were performed in the presence (+*IHF*; 30 nM) or absence (−*IHF*) of IHF with supercoiled plasmid DNA templates of superhelical density $\sigma = -0.07$ as described under "Materials and Methods." Transcription reactions were terminated after 2, 4, 6, 8, and 10 min, and the 157-nucleotide *ilv*P_G transcript was isolated by electrophoresis on a denaturing 8% polyacrylamide gel containing 8 M urea and visualized by autoradiography. The 229-nucleotide *ilv*P_G1 transcript arises from a fortuitous *in vitro* promoter in the A + T-rich UAS1 region present in the plasmid pDHΔwt but not in plasmid pSSΔ-98. Transcription from this promoter is repressed in the presence of IHF. The doublet transcription product bands are presumed to arise from heterogeneous termination. *B*, data obtained from the above *in vitro* transcription reactions were plotted, and the rate of transcript formation was determined by the slope of *ilv*P_G-specific band intensity *versus* time in minutes. -Fold activation was determined by dividing the rate of transcription in the presence of IHF by the transcription rate in the absence of IHF

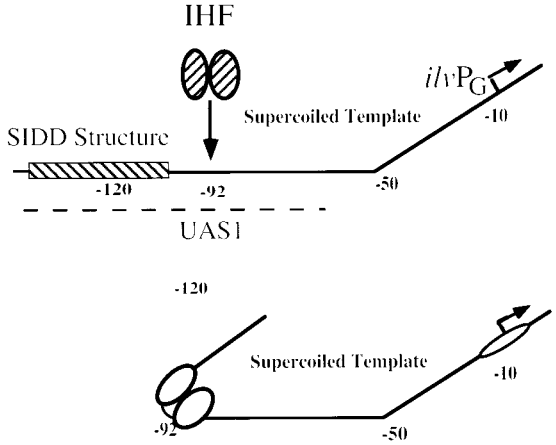

FIG. 10. **DNA structural transmission (competing structural transitions) mechanism of DNA superhelix-dependent transcriptional activation of the *ilv*P_G promoter by IHF.** See text for discussion.

ble that this downstream destabilization was caused by the IHF-induced inhibition of transitions in the upstream UAS1 region. If this hypothesis is correct, then no activation would be expected in the absence of this structure. Since the region that experiences this destabilization is upstream from the IHF binding site in UAS1 (Figs. 1 and 3), it was possible to replace it with a superhelically stable DNA sequence without affecting the DNA sequence of the IHF binding and promoter sites (Fig. 5) or the ability of IHF to bind to its target site in the UAS1 region (Fig. 8). When this superhelically destabilized DNA sequence in UAS1 was replaced with a superhelically stable one, it was observed that, as expected, IHF could not activate transcription initiation from the *ilv*P_G promoter, even on a highly supercoiled DNA template (Fig. 9). Furthermore, in the absence of the superhelically destabilized structure in UAS1, IHF binding to a supercoiled DNA template does not destabilize the DNA duplex in the −10 region of the downstream *ilv*P_G promoter (Fig. 7). These results demonstrate that IHF-mediated inhibition of the formation of this structure is responsible for the downstream duplex destabilization that leads to activation of transcription initiation from the *ilv*P_G promoter.

This DNA structural transmission mechanism further predicts that the threshold superhelical densities required for duplex destabilization in the UAS1 region and for IHF activation of transcription initiation from the *ilv*P_G promoter should be similar. No transmission would be expected at less extreme superhelical stress levels than those required for duplex destabilization in UAS1. Two-dimensional gel electrophoresis of topoisomer sets of the pDHΔwt plasmid containing the *ilv*P_G promoter-regulatory region suggest that this is the case. Negative superhelical densities of $\sigma > -0.032 \pm 0.003$ are required for duplex destabilization in the UAS1 region of this plasmid (Figs. 4 and 6). This value agrees well with our previously

estimated threshold negative superhelical density of $\sigma > -0.035 \pm 0.005$ for IHF activation (8). It should be emphasized, however, that these values are not expected to be identical. This is because the conditions required for each of these measurements are different. The two-dimensional gel experiments were performed at a lower ionic strength (45 mM Tris borate) than the transcription reactions (100 mM KCl). Stable unwinding of A + T-rich regions is known to be suppressed at ionic strengths greater than 50 mM NaCl (16). Thus, a negative superhelical density more extreme than the threshold value measured by the two-dimensional electrophoresis experiment is expected in a transcription reaction that occurs at a higher salt concentration. On the other hand, destabilization of the UAS1 region at a less extreme threshold is predicted by the fact that additional negative supercoiling is generated in this region during basal level transcription from the downstream *ilv*P_G promoter (17–19). For example, Rahmouni and Wells (20) have shown the formation of a supercoiling-dependent B-DNA to Z-DNA transition upstream of an active promoter, although the average superhelical density present *in vivo* should not have been high enough to induce this structural transition (19).

It has been documented that small sequence changes can radically alter the transition behavior of a supercoiled molecule if they change the relative competitiveness of different regions (5). Two examples of this behavior are relevant to this report. First, deleting a portion (even a small portion) of a strongly destabilized site can radically alter its competitiveness, causing the transition to shift to another location although most of the original site remains intact. In the case described here, removal of part of the UAS1 region destroys the ability of the remaining downstream promoter portion to become destabilized by superhelicity. Second, it is possible to alter transition behavior by constraining a portion of an easily destabilized DNA region to remain in the B-form. This also can have the effect of altering the competitiveness of the region involved sufficiently to shift the transition to another part of the same destabilized region or to another easily destabilized site. This is the essence of the mechanism proposed in this report; *i.e.* IHF binding forces the superhelically destabilized site in the UAS1 region to remain in the B-form, which shifts part of the transition energy to the promoter site of this SIDD region and the rest to other easily destabilized sites.

Another IHF-mediated, supercoiling-dependent model for the regulation of transcription has been reported. Higgins *et al*. (34) have suggested that IHF activates transcription from the phage μ P_E promoter by forcing the promoter site to the outside of a superhelical node where it is in an ideal location for interaction with RNA polymerase. In support of this model, Van Rijn *et al*. (35) demonstrated that this activation is dependent on the face of the helix and correlated with increased RNA polymerase binding affinity. In contrast, the IHF-mediated activation of transcription from the *ilv*P_G promoter is independent of the face of the helix and affects the kinetic step of open complex formation (7). Thus, a super-loop type model can be excluded for IHF-mediated regulation of transcription from the *ilv*P_G promoter. It was also noted that both IHF binding in the UAS1 region and the pSSΔ-98 construct eliminate *in vitro* transcription from the *ilv*P_G1 promoter (Fig. 9). This suggested the possibility that IHF might act to facilitate downstream promoter selection by repressing transcription from the upstream promoter. However, previously published data demonstrate that this is also not the case (7). Point mutations in the UAS1 region that abolish transcription from *ilv*P_G1 but do not affect IHF-binding do not activate transcription from the downstream *ilv*P_G promoter. Furthermore, these point mutations do not affect IHF-mediated activation.

It is of interest to note that DNA sequences having higher than average A + T content are observed upstream of several strong σ^{70} promoters and that alterations in these upstream A + T-rich regions affect the rates of transcription initiation from downstream promoters (21, 22). Since a considerable proportion of the negative supercoiling in the bacterial nucleoid is unconstrained, these A + T-rich regions can serve as local sites that are susceptible to destabilization. The results reported here demonstrate that regulatory proteins that bind to these upstream regions can affect the susceptibility of sequences to become destabilized by imposed superhelicity and transfer this susceptibility to nearby promoter sites. Therefore, the mechanism of protein-mediated, superhelicity-dependent, regulation of transcription initiation in prokaryotes that is reported here may be of general significance. For example, Fyfe and Davies (36) have recently reported that the deletion of an A + T-rich DNA sequence upstream of an IHF binding in the regulatory region of the *Neisseria gonorrhoreae pilE*p_1 promoter, which has a striking resemblance to the *ilv*P_G promoter-regulatory region described here, eliminates IHF-mediated activation in this system. However, the DNA supercoiling dependence of this activation has not yet been examined.

Recent reports indicate that DNA superhelicity and superhelically destabilized structures also are important for the regulation of transcription in eukaryotes. For example, Emerson and colleagues (23) have shown that supercoiled DNA templates are required for enhancer-mediated *in vitro* regulation of the chicken β^A-globin and mouse T-cell receptor genes. Also, Michelotti *et al.* (24) have shown that the basal level of transcription from the *c-myc* gene generates negative DNA superhelicity that destabilizes upstream A + T sequences. These destabilized regions are targets for single-stranded DNA-binding proteins that are required for enhanced *in vivo* transcription from this promoter. Thus, it appears that protein-stabilized DNA duplex destabilization might serve a range of roles in *in vivo* regulatory mechanisms in both prokaryotes and eukaryotes.

In conclusion, it should be stressed that it is essential to separate the strands of the DNA duplex for many biological processes such as DNA replication, recombination, and transcription initiation in both prokaryotes and eukaryotes (25–27). Negative superhelicity lowers the energy of activation for strand separation. The data presented in this report demonstrate a level of regulation for these processes that involves a competition between potential destabilized sites that is mediated by protein binding. Therefore, since it is now apparent that DNA supercoiling is an integral component of many mechanisms involved in the regulation of cell growth and metabolism, a further elucidation of these types of protein-mediated, DNA supercoiling-dependent effects should enhance our understanding of a large number of regulatory systems.

Acknowledgments—We are grateful to Elaine Ito for technical assistance and to Stuart Arfin, She-Pin Hung, and our colleagues at the University of California, Irvine, for helpful discussions.

REFERENCES

1. Benham, C. J. (1992) *J. Mol. Biol.* **225,** 835–847
2. Aboul-ela, F., Bowater, R. P., and Lilley, D. M. (1992) *J. Biol. Chem.* **267,** 1776–1785
3. Kowalski, D., Natale, D. A., and Eddy, M. J. (1988) *Proc. Natl. Acad. Sci. U. S. A.* **85,** 9464–9468
4. Benham, C. J. (1979) *Proc. Natl. Acad. Sci. U. S. A.* **76,** 3870–3874
5. Benham, C. J. (1996) *J. Mol. Biol.* **255,** 425–434
6. Pagel, J. M., Winkelman, J. W., Adams, C. W., and Hatfield, G. W. (1992) *J. Mol. Biol* **224,** 919–935
7. Parekh, B. S., and Hatfield, G. W. (1996) *Proc. Natl. Acad. Sci. U. S. A.* **93,** 1173–1177
8. Parekh, B. S., Sheridan, S. D., and Hatfield, G. W. (1996) *J. Biol. Chem.* **271,** 20258–20264
9. Lawther, R. P., Wek, R. C., Lopes, J. M., Pereira, R., Taillon, B. E., and Hatfield, G. W. (1987) *Nucleic Acids Res.* **15,** 2137–2155

10. Benham, C. J. (1993) *Proc. Natl. Acad. Sci. U. S. A.* **90,** 2999–3003
11. Palecek, E. (1992) *Methods Enzymol.* **212,** 139–155
12. Bowater, R., Aboul-ela, F., and Lilley, D. M. J. (1992) *Methods Enzymol.* **212,** 105–119
13. Shindo, H., Kanke, F., Miyake, M., Matsumoto, U., and Shimizu, M. (1995) *Biol. Pharm. Bull.* **18,** 1328–1334
14. Friedman, D. I. (1988) *Cell* **55,** 545–554
15. Rice, P. A., Yang, S., Mizuuchi, K., and Nash, H. A. (1996) *Cell* **87,** 1295–1306
16. Bowater, R. P., Aboul-ela, F., and Lilley, D. M. (1994) *Nucleic Acids Res.* **22,** 2042–2050
17. Wu, H. Y., Shyy, S. H., Wang, J. C., and Liu, L. F. (1988) *Cell* **53,** 433–440
18. Liu, L. F., and Wang, J. C. (1987) *Proc. Natl. Acad. Sci. U. S. A.* **84,** 7024–7027
19. Rahmouni, A. R., and Wells, R. D. (1992) *J. Mol. Biol.* **223,** 131–144
20. Rahmouni, A. R., and Wells, R. D. (1989) *Science* **246,** 358–363
21. Nishi, T., and Itoh, S. (1986) *Gene* (*Amst.*) **44,** 29–36
22. Haughn, G. W., Wessler, S. R., Gemmill, R. M., and Calvo, J. M. (1986) *J. Bacteriol.* **166,** 1113–1117
23. Barton, M. C., Madani, N., and Emerson, B. M. (1997) *Proc. Natl. Acad. Sci. U. S. A.* **94,** 7257–7262
24. Michelotti, G. A., Michelotti, E. F., Pullner, A., Duncan, R. C., Eick, D., and Levens, D. (1996) *Mol. Cell. Biol.* **16,** 2656–2669
25. Pruss, G. J., and Drlica, K. (1989) *Cell* **56,** 521–523
26. Drlica, K. (1992) *Mol. Microbiol* **6,** 425–433
27. Steck, T. R., Franco, R. J., Wang, J. Y., and Drlica, K. (1993) *Mol. Microbiol.* **10,** 473–481
28. Nash, H. A., Robertson, C. A., Flamm, E., Weisberg, R. A., and Miller, H. I. (1987) *J. Bacteriol.* **169,** 4124–4127
29. Sambrook, J., Fritsch, E. F., and Maniatis, T. (1989) *Molecular Cloning: A Laboratory Manual*, 2nd Ed., Cold Spring Harbor Laboratory, Cold Spring Harbor, New York
30. Ausubel, F., Brent, R., Kingston, R. E., Moore, D. D., Siedman, J. G., Smith, J. A., and Struhl, K. (1993) *Current Protocols in Molecular Biology*, Greene Publishing Associates, Inc. and John Wiley & Sons, Inc., New York
31. Keller, W. (1975) *Proc. Natl. Acad. Sci. U. S. A.* **72,** 4876–4880
32. Singleton, C. K., and Wells, R. D. (1982) *Anal. Biochem* **122,** 253–257
33. Benham, C. J. (1990) *J. Chem. Phys.* **92,** 6294–6305
34. Higgins, N. P., Collier, D. A., Kilpatrick, M. W., and Krause, H. M. (1989) *J. Biol. Chem.* **264,** 3035–3042
35. van Rijn, P. A., Goosen, N., van de Putte, P. (1988) *Nucleic Acids Res.* **16,** 4595–4605
36. Fyfe, J. A. M., and Davies, J. K. (1998) *J. Bacteriol.* **180,** 2152–2159